ChemComm

Chemical Communications

rsc.li/chemcomm

ROYAL SOCIETY OF CHEMISTRY
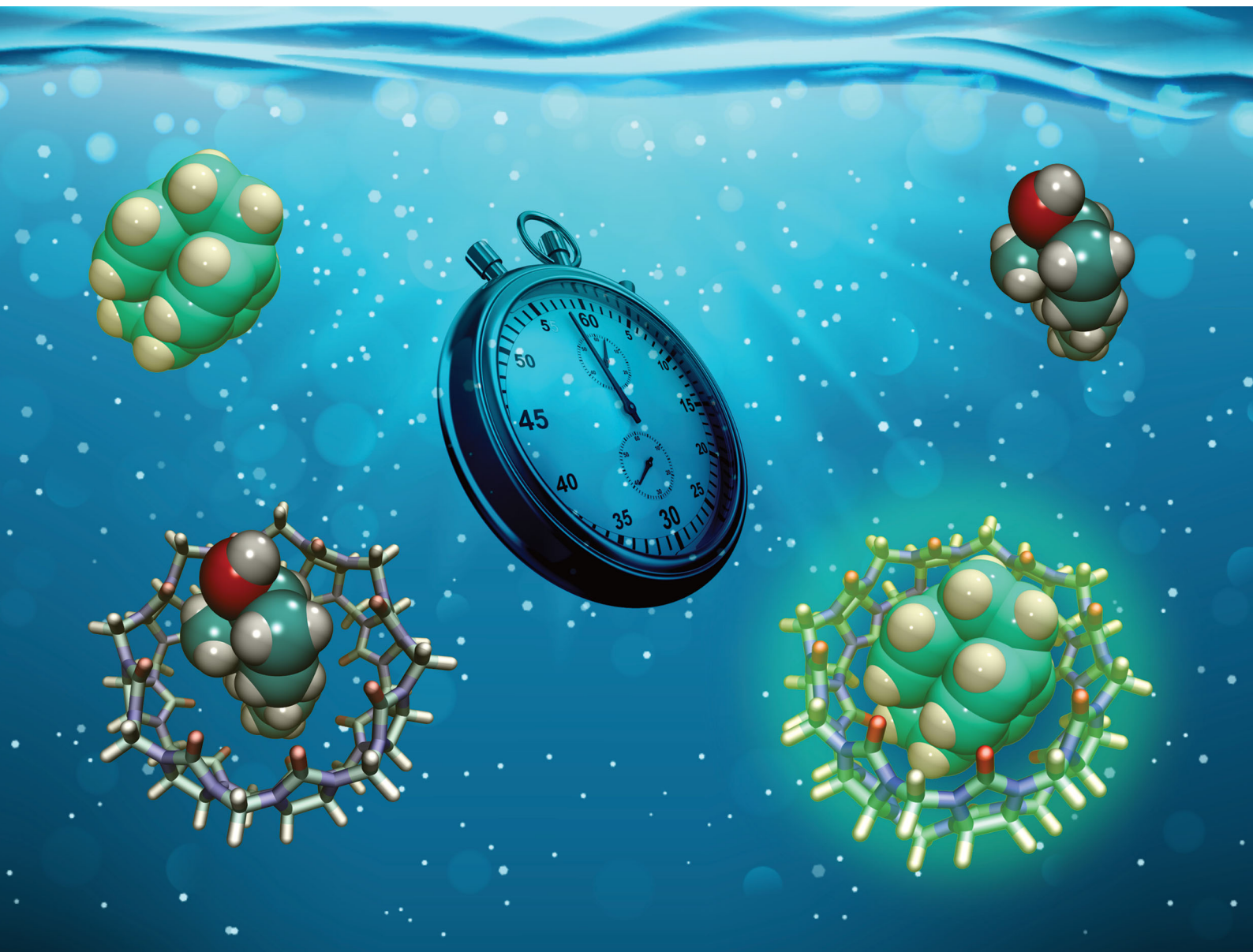
COMMUNICATION
Stephan Sinn, Frank Biedermann *et al.*
Teaching indicators to unravel the kinetic features of
host–guest inclusion complexes

Check for updates

Teaching indicators to unravel the kinetic features of host–guest inclusion complexes†

Amrutha Prabodh, [a] Stephan Sinn, *[a] Laura Grimm, [a] Zsombor Miskolczy, [b] Mónika Megyesi, [b] László Biczók, [b] Stefan Bräse [cd] and Frank Biedermann *[a]

Both thermodynamic and kinetic insights are needed for a proper analysis of association and dissociation processes of host–guest interactions. However, kinetic descriptions of supramolecular systems are scarce in the literature because suitable experimental protocols are lacking. We introduce here three time-resolved methods that allow for convenient determination of kinetic rate constants of spectroscopically silent or even insoluble guests with the macrocyclic cucurbit[n]uril family and human serum albumin (HSA) protein as representative hosts.

It has become clear that not only thermodynamic characteristics, *e.g.*, binding affinities, but also the assessment of kinetic parameters (*e.g.*, complexation and decomplexation rates) is required to obtain a full picture of supramolecular systems.[1–4] For instance, kinetic rate constants of supramolecular complexes are key parameters for understanding catalysis[5] and protein–ligand binding mechanisms,[6–9] and stimuli-responsive materials.[10,11] The design of out-of-equilibrium systems also requires knowledge of both K_a values and rate constants.[12–15] However, except for CEST-active[3] or slowly equilibrating systems that can be monitored by NMR (*e.g.*, DOSY, EXSY, inversion recovery),[1,16–20] kinetic rate constants of supramolecular systems are experimentally mostly only available for chromophoric or emissive systems.[2,4,21–23] These experiments are typically conducted as time-resolved direct host–guest binding titration assays, herein abbreviated as *kin*DBA (Fig. 1a). In some cases, single molecule measurements with nanopores allowed for assessing the kinetic rate constants for complexation and decomplexation of entrapped host–guest complexes.[15,24,25]
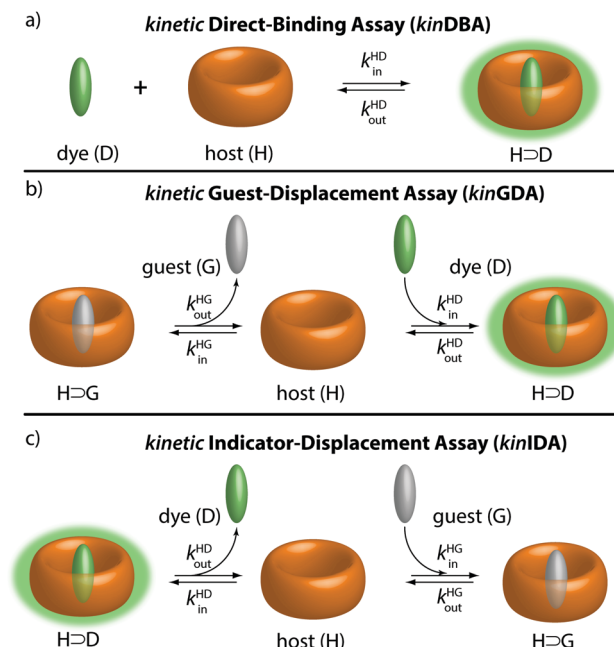
[a] Karlsruhe Institute of Technology (KIT), Institute of Nanotechnology (INT), Hermann-von-Helmholtz-Platz 1, 76344 Eggenstein-Leopoldshafen, Germany. E-mail: stephan.sinn@kit.edu, frank.biedermann@kit.edu

[b] Institute of Materials and Environmental Chemistry Research Centre for Natural Sciences, Magyar tudósok körútja 2, 1117 Budapest, Hungary

[c] Karlsruhe Institute of Technology (KIT), Institute of Organic Chemistry (IOC), Fritz-Haber-Weg 6, 76131 Karlsruhe, Germany

[d] Institute of Biological and Chemical Systems – Functional Molecular Systems (IBCS-FMS), Hermann-von-Helmholtz-Platz 1, 76344 Eggenstein-Leopoldshafen, Germany

† Electronic supplementary information (ESI) available: Materials and methods, experimental details, as well as fitting equations. See DOI: 10.1039/d0cc03715j

Fig. 1 Working principles of supramolecular assays for the determination of complexation rates (k_{in}) and decomplexation rates (k_{out}) of host–guest complexes. (a) Known direct-binding assay that is limited to spectroscopically active host or guests. (b) and (c) Herein introduced competitive kinetic guest-displacement-assay (*kin*GDA) and kinetic indicator-displacement-assay (*kin*IDA) that are applicable also to spectroscopically silent guests.

Conversely, binding affinities (K_a) of host–guest complexes can be obtained for a wide range of hosts and guests by several different techniques, for instance, through NMR titrations and calorimetric measurements (ITC) as representative direct-binding assays[26–28] or competitive-binding assays such as the indicator-displacement assay (IDA)[28,29] and the recently by us introduced guest-displacement assay (GDA).[30] Consequently, there is a strong mismatch between the number of reported binding affinities and kinetic parameters for any class of host–guest complexes. For instance, a survey for the cucurbit[n]uril (CB*n*)[31,32] macrocyclic hosts (see Fig. 2 for their structure) on the
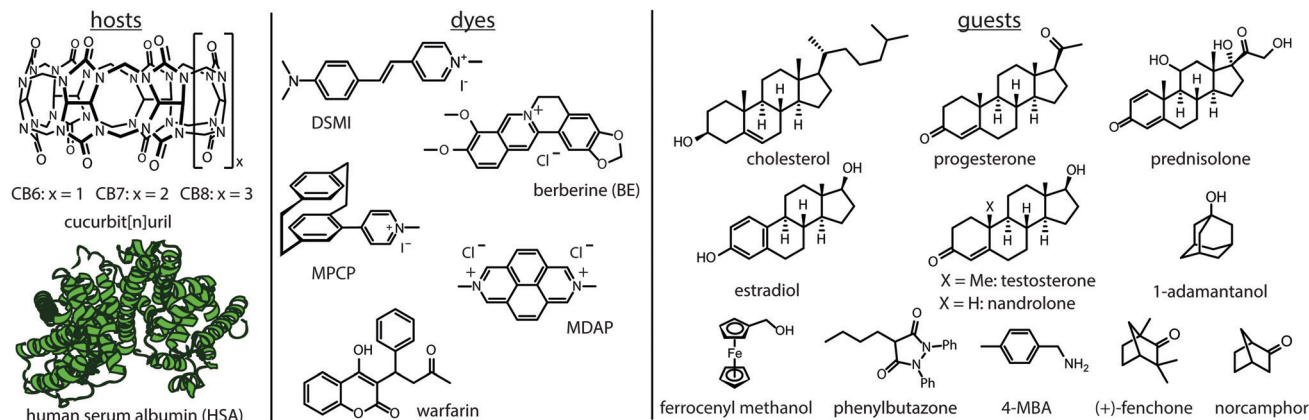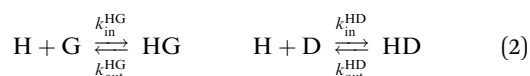
Fig. 2 Chemical structures of hosts, fluorescent indicator dyes, and guests used in this study.

supramolecular repository "SupraBank.org" revealed that only 3% of all entries for CB*n*–guest complexes included also kinetic rate constants, in agreement with the much larger number of K_a values *versus* kinetic parameters tabulated in reviews.

Herein, we show three novel competitive approaches through which kinetic rate constants of host–guest complexes, namely the complexation rate (k_{in}) and decomplexation rate (k_{out}) constants, can be accessed for spectroscopically silent guests. A competitive binding network consisting of a host (H), guest (G), and indicator dye (D) – see Fig. 1 – can be described both by thermodynamic[30] and by kinetic equations (see ESI† for details). The binding affinities of the host-dye (H⊃D) and host–guest (H⊃G) complex are denoted as K_a^{HD} and K_a^{HG}, respectively. The complexation & decomplexation rate constants of the H⊃D and H⊃G complexes are symbolised by k_{in}^{HD} & k_{out}^{HD} and k_{in}^{HG} & k_{out}^{HG}, respectively. Note that an "S_N1"-type, *i.e.*, purely dissociative mechanism for the decomplexation step of the H⊃G and H⊃D complexes is implied by kinetic eqn (1)–(3).

$$HG + D \rightleftarrows HD + G \qquad (1)$$

$$H + G \underset{k_{out}^{HG}}{\overset{k_{in}^{HG}}{\rightleftarrows}} HG \qquad H + D \underset{k_{out}^{HD}}{\overset{k_{in}^{HD}}{\rightleftarrows}} HD \qquad (2)$$

$$K_a^{HD} = k_{in}^{HD}/k_{out}^{HD} \qquad K_a^{HG} = k_{in}^{HG}/k_{out}^{HG} \qquad (3)$$

$$I_t = I^0 + I^{HD}\cdot[HD]_t + I^D\cdot[D]_t \qquad (4)$$

Eqn (3) shows how the thermodynamic and kinetic parameters, *i.e.*, affinity and rate constants, are coupled to each other. The mathematical expression for the background-corrected observable signal intensity I_t at time t is given by eqn (4), assuming that both the host and guest are spectroscopically silent. To kinetically characterize a supramolecular host–guest complex, it is, therefore, the task to obtain k_{in}^{HG} & k_{out}^{HG} by fitting an experimentally obtained signal-time curve of a non-equilibrated competitive binding network involving the host, guest, and dye.

The first, a conceptionally most intuitive method introduced here is the time-resolved guest-displacement assay, *kin*GDA. Fig. 3a shows the *kin*GDA traces that were obtained when the ultra-high-affinity dye MPCP[33] was added to a solution of
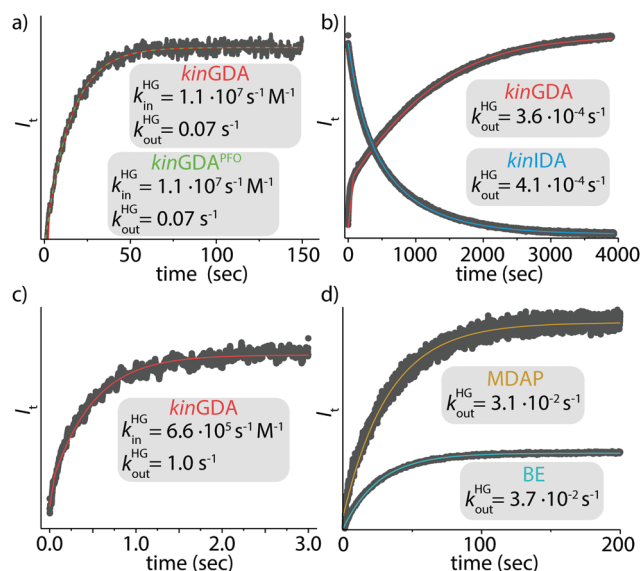

Fig. 3 Kinetic traces of (a) CB8⊃nandrolone (1 μM) and MPCP (50 μM) (●, — fitting for *kin*GDA and — fitting for *kin*GDA^PFO), (b) CB7, nandrolone and BE (all 2 μM) either in *kin*GDA (●, — fitting) or *kin*IDA (●, — fitting) mode, (c) HSA (20 μM), PBZ (40 μM) and warfarin (100 μM) in PBS in *kin*GDA mode (●, — fitting), (d) CB7 (2 μM), nandrolone (2 μM) and MDAP (25 μM, ●, — fitting) or BE (50 μM, ●, — fitting), in sodium phosphate buffer (50 mM) in *kin*GDA^PFO mode. T = 25 °C. See ESI† for details.

spectroscopically silent CB8⊃nandrolone complex. During the re-equilibration, nandrolone leaves the CB8 cavity, making room for the inclusion of indicator dye MPCP, which is the stronger binding guest. The detectable rate depends on (i) the concentrations of the host, guest, and dye, (ii) the rate constants k_{in}^{HD} and k_{out}^{HD} of the dye, which can be determined by a kinetic direct-binding assay (*kin*DBA) (see Table S3 and Fig. S2, S6–S8, S18, S24, S28, and S33, ESI†), and (iii) on the unknown rate constants k_{in}^{HG} and k_{out}^{HG} of the spectroscopically silent guest. The rate constants k_{in}^{HG} and k_{out}^{HG} can then be extracted from the time-resolved *kin*GDA curves through a mathematical fitting. Because the goodness of the fit improves when $K_a^{HG} = k_{in}^{HG}/k_{out}^{HG}$ is used as an input parameter, prior K_a^{HG} determination, *e.g.*, through competitive binding titrations such as GDA or IDA or direct

Table 1 Experimental k_{in}, k_{out} and log K_a for host–guest and protein–ligand complexes determined by kinGDA, kinIDA and kinGDA^{PFO} in aqueous media

Guest[a]	Host[a]	k_{in}^{HG}/s^{-1} M^{-1}	k_{out}^{HG}/s^{-1}	Method[b]	log (K_a/M^{-1})
4-MBA	CB6[c]	3.3×10^4	6.5×10^{-4}	kinIDA[d]	7.7[e]
Cholesterol	CB7[f]	7.0×10^4	8.7×10^{-2}	kinGDA[g]	5.9[h]
		7.0×10^4	8.7×10^{-2}	kinGDA^{PFO} [g]	
Estradiol	CB7	4.2×10^4	2.0×10^{-2}	kinGDA[g]	6.3[h]
		4.3×10^4	2.1×10^{-2}	kinGDA^{PFO} [g]	
(+)-Fenchone	CB7[i]	9.2×10^4	3.2×10^{-3}	kinGDA[g]	7.5[e]
Norcamphor	CB7[i]	1.5×10^7	9.8×10^{-2}	kinGDA[g]	8.2[e]
Adamantanol	CB7[j]	1.7×10^5	6.6×10^{-6}	kinIDA[g]	10.4[e]
	CB8[j]	1.2×10^7	1.97	kinGDA[k]	6.8[l]
		1.2×10^7	1.92	kinGDA^{PFO} [k]	
Nandrolone[m]	CB7[n]	4.1×10^3	3.6×10^{-4}	kinGDA[g]	7.1[o]
		4.5×10^3	4.1×10^{-4}	kinIDA[g]	
	CB7[p]	2.3×10^3	2.0×10^{-4}	kinGDA[g]	7.1[o]
		2.4×10^3	2.1×10^{-4}	kinGDA^{PFO} [g]	
	CB7[q]	(9×10^3)	(8×10^{-4})	kinGDA[t]	7.1[o]
		(9×10^3)	(8×10^{-4})	kinGDA^{PFO} [t]	
	CB7[r]	3.0×10^3	3.7×10^{-2}	kinGDA^{PFO} [g]	5.2[s]
		2.5×10^3	3.1×10^{-2}	kinGDA^{PFO} [t]	
	CB8	1.1×10^7	6.8×10^{-2}	kinGDA[k]	8.2[h]
		1.1×10^7	7.1×10^{-2}	kinGDA^{PFO} [k]	
Prednisolone	CB8	1.6×10^6	1.1	kinGDA[k]	6.2[o]
		1.5×10^6	1.1	kinGDA^{PFO} [k]	
Testosterone	CB8	6.4×10^5	5.8×10^{-3}	kinGDA[k]	8.0[o]
		6.4×10^5	5.8×10^{-3}	kinGDA^{PFO} [k]	
Ferrocenyl methanol	CB8[j]	2.1×10^7	5.8	kinGDA[k]	6.6[l]
		2.0×10^7	5.7	kinGDA^{PFO} [k]	
Phenylbutazone	HSA[u]	6.6×10^5	1.0	kinGDA[v]	5.8[h]

Errors (StDev) from triplicate experiments are ≤30% in k_{in}^{HG} and k_{out}^{HG}, see Table S3 (ESI). If not stated otherwise experiments were conducted in deionized water at 25 °C. Minor to no differences in guest binding kinetics have been found for non-desalted and desalted hosts. [a] See Fig. 2 for chemical structures. [b] See Table S3 (ESI) for indicator kinetics. [c] In deionized water with 8.23 μM HCl. [d] DSMI as dye. [e] See ESI for details. [f] H$_2$O/ethanol (99.9/0.1; v/v) mixture. [g] BE as dye. [h] See ref. 30. [i] In water freshly distilled three times from dilute KMnO$_4$ solution. [j] Desalted CB7/CB8. [k] MPCP as dye. [l] Determined by ITC. [m] CB7 (2 μM), nandrolone (log (K_a^{HG}/M^{-1}) = 7.04;[40] 2 μM). [n] Dye (2 μM). [o] See ref. 40. [p] Dye (50 μM). [q] Dye (40 μM) likely associative mechanism also present, see text. [r] BE (50 μM) or MDAP (25 μM) in sodium phosphate buffer (50 mM). [s] Calculated using the formula presented in ref. 41. [t] MDAP as dye. [u] In phosphate buffered saline (PBS). [v] Warfarin as dye.

binding assays (DBA) is recommended. Several host–guest pairs (Fig. S1–S34, ESI†) were analysed in this way, see Table 1. Note that the kinGDA method is extendable for determining the decomplexation rates of insoluble guests such as estradiol through precomplexation, e.g., see Table 1 for the rate constants k_{in}^{HG} and k_{out}^{HG} for the CB7 ⊃ estradiol complex and Fig. S16 (ESI†) for the kinetic trace and fit. The applicability of kinGDA to insoluble guests is an asset it shares with the thermodynamic GDA method.[30] The concept is transferable to protein–ligand interactions, as exemplified for human serum albumin (HSA) as a biological important carrier protein[31,32] that is commercially available.[35,36] Fig. 3c demonstrates the determination of the kinetic rate constants for the binding of the anti-inflammatory drug phenylbutazone[34,35] (PBZ) to HSA by kinGDA.

The second competitive kinetic method, the pseudo-first order kinGDA (kinGDA^{PFO}), has a close analogy to some literature reports,[18,36] and allows for measuring k_{out}^{HG} values without explicit knowledge of the kinetic rate constants of the indicator dye. Firstly, host and guest are equilibrated, followed by the spiked addition of excess of a high-affinity dye. Use of excess of the indicator allows for decoupling guest and dye rate constants for (de)complexation through a pseudo-first order approximation (see eqn (S15)–(S22), ESI†).

The kinetic trace is recorded and then fitted by a simple exponential decay function

$$I_t = I^{eq} + A \cdot e^{-tk_{out}^{HG}} \qquad (5)$$

to yield the kinetic parameter k_{out}^{HG} of interest (I^{eq} – signal offset at equilibration to HD; A – amplitude). The k_{in}^{HG} value is then obtained from $k_{in}^{HG} = k_{out}^{HG} \cdot K_a^{HG}$. In kinGDA^{PFO}, knowledge of the exact concentrations of the involved partners is not needed, thus, kinGDA^{PFO} can often be the practical choice. However, it is important to note that the applicability of kinGDA^{PFO} is restricted because $k_{in}^{HG}[G]_0 \ll k_{in}^{HD}[D]_0$ is required. Ideally, the kinGDA^{PFO} traces should overlay upon varying the dye concentration, excluding concentration-induced changes in the binding mechanisms. For most of the CBn–guest complexes, we found that the kinGDA^{PFO} method is applicable. However, the high dye concentrations required for kinGDA^{PFO} can cause undesirable associative-binding contributions to H ⊃ G decomplexation mechanism. For example, at higher concentrations the dicationic MDAP may form a (transient) ternary complex with charge-neutral CB7 ⊃ nandrolone in deionized water, causing an apparent increase in k_{out} (Table 1). This scenario is plausible because the decomplexation rate of CB7 ⊃ nandrolone strongly increased in phosphate buffer (Fig. 3d), which implies formation of ternary M^{n+}·CB7 ⊃ nandrolone complexes. (See ref. 37–39 for precedence for M^{n+}·CBn ⊃ G complexes). Thus, ternary dye·CB7 ⊃ guest complexes are likely not present in buffered or saline aqueous media and the high dye concentration needed for the kinGDA^{PFO} method is of no concern (see Table 1).

Finally, a third competitive method, the time-resolved indicator displacement assay (kinIDA), can be employed for obtaining kinetic rate constants. In kinIDA, a pre-equilibrated host-dye pair is mixed with the guest, to which the binding network responds with dye displacement (Fig. 1c). Indeed, comparable results were obtained for kinIDA and kinGDA for the system composed of nandrolone (G), CB7 (H) and berberine (D), see Fig. 3b.

The kinetic methods introduced herein provide meaningful rate constants if the host–guest and host-dye displacement mechanism follow a strict dissociative and not an additional, occasionally observed,[36] associative mechanism. Several tests can be adopted to validate a dissociative mechanism. (i) kinGDA can be conducted at different dye concentrations and should yield similar k_{in}^{HG} and k_{out}^{HG} parameters. (ii) The kinGDA method can be compared to the analogous kinIDA setup, see above. In many cases, the competitive methods can circumvent the need for stopped-flow equipment because the equilibration times in the competitive assay format are much longer than in kinDBA. Thus, kinetic characterizations of CBn–guest complexes can now also be conducted in laboratories that do not have access to specialized stopped-flow setups. For instance, the kinetic rate constants for the CB7 ⊃ steroid and CB8 ⊃ steroid complexes can

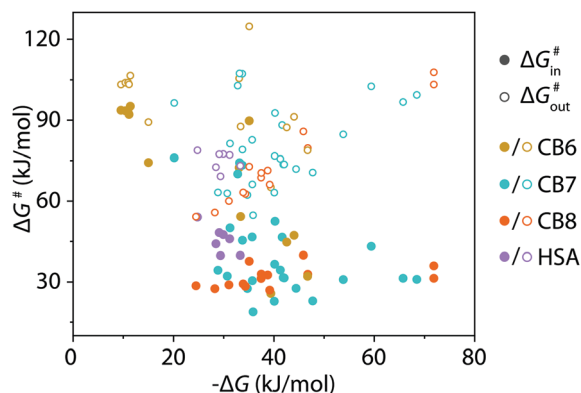Fig. 4 Correlation plot of Gibb's free energy (ΔG) of complex formation *versus* Gibb's energy of activation ($\Delta G^{\#}$) for complexation ($\Delta G_{in}^{\#}$) and decomplexation ($\Delta G_{out}^{\#}$). Values were calculated from acquired and literature data (see ESI†) for CB6−8 and HSA.

be determined in a cuvette equipped with a magnetic stirrer by a standard fluorescence spectrometer. Conversely, explorative *kin*GDA and *kin*IDA experiments for β-cyclodextrin complexes with high-affinity guests such as adamantanol resulted in equilibration times that were even too fast (<100 ms at 298 K) for our stopped-flow setup. The investigations of CB*n* complexes and the protein–ligand complex HSA⊃PBZ show that *kin*GDA, *kin*GDA^{PFO}, and *kin*IDA yield reliable fits for guest egression rates $k_{out}^{HG} \leq 10$ s^{-1}. The kinetic rate constants that became available through the use of presented methods were converted alongside literature data to Gibb's activation energies by Eyring's equation, see also eqn (S24), (S25) and Table S4 in the ESI.† The data displayed in Fig. 4 shows a clear decoupling of thermodynamic and kinetic features for the CB*n*–guest and HSA–guest complexes compiled, motivating future in-depth analysis of these host–guest inclusion complexes. A first assessment demonstrates that increased thermodynamic stability is not always correlated to an increase in the kinetic inertness of the CB*n*–guest complexes. In conclusion, it was shown that *kin*IDA, *kin*GDA, and *kin*GDA^{PFO} provide an experimental assessment of kinetic rate constants of spectroscopically silent host–guest and protein–ligand pairs. These methods will find use in the supramolecular and protein community due to their ease and scope.

Conflicts of interest

There are no conflicts of interest to declare.

Notes and references

1 C. Marquez, R. R. Hudgins and W. M. Nau, *J. Am. Chem. Soc.*, 2004, **126**, 5806–5816.
2 C. Bohne, *Chem. Soc. Rev.*, 2014, **43**, 4037–4050.
3 L. Avram, A. D. Wishard, B. C. Gibb and A. Bar-Shir, *Angew. Chem. Int. Ed.*, 2017, **56**, 15314–15318.
4 E. Masson, M. Raeisi and K. Kotturi, *Isr. J. Chem.*, 2018, **58**, 413–434.
5 K. I. Assaf and W. M. Nau, *Chem. Soc. Rev.*, 2015, **44**, 394–418.
6 H. J. Motulsky and L. C. Mahan, *Mol. Pharmacol.*, 1984, **25**, 1.
7 R. Casasnovas, V. Limongelli, P. Tiwary, P. Carloni and M. Parrinello, *J. Am. Chem. Soc.*, 2017, **139**, 4780–4788.
8 M. Bernetti, A. Cavalli and L. Mollica, *MedChemComm*, 2017, **8**, 534–550.
9 P. J. Tonge, *ACS Infect. Dis.*, 2019, **5**, 796–808.
10 E. A. Appel, J. del Barrio, X. J. Loh and O. A. Scherman, *Chem. Soc. Rev.*, 2012, **41**, 6195–6214.
11 X. Yan, F. Wang, B. Zheng and F. Huang, *Chem. Soc. Rev.*, 2012, **41**, 6042–6065.
12 J. J. Armao IV and J.-M. Lehn, *Angew. Chem. Int. Ed.*, 2016, **55**, 13450–13454.
13 G. Ashkenasy, T. M. Hermans, S. Otto and A. F. Taylor, *Chem. Soc. Rev.*, 2017, **46**, 2543–2554.
14 J. H. van Esch, R. Klajn and S. Otto, *Chem. Soc. Rev.*, 2017, **46**, 5474–5475.
15 S. Borsley, J. A. Cooper, P. J. Lusby and S. L. Cockroft, *Chem. – Eur. J.*, 2018, **24**, 4542–4546.
16 D. J. Cram and G. M. Lein, *J. Am. Chem. Soc.*, 1985, **107**, 3657–3668.
17 A. Wu and L. Isaacs, *J. Am. Chem. Soc.*, 2003, **125**, 4831–4835.
18 J. S. Mugridge, R. G. Bergman and K. N. Raymond, *Angew. Chem. Int. Ed.*, 2010, **49**, 3635–3637.
19 T. J. Williams, A. D. Kershaw, V. Li and X. Wu, *J. Chem. Educ.*, 2011, **88**, 665–669.
20 T. Rama, E. M. Lopez-Vidal, M. D. Garcia, C. Peinador and J. M. Quintela, *Chemistry*, 2015, **21**, 9482–9487.
21 Z. Miskolczy, L. Biczok and I. Jablonkai, *Phys. Chem. Chem. Phys.*, 2017, **19**, 766–773.
22 E. A. Appel, F. Biedermann, D. Hoogland, J. Del Barrio, M. D. Driscoll, S. Hay, D. J. Wales and O. A. Scherman, *J. Am. Chem. Soc.*, 2017, **139**, 12985–12993.
23 S. S. Thomas, H. Tang and C. Bohne, *J. Am. Chem. Soc.*, 2019, **141**, 9645–9654.
24 S. Borsley, M. M. Haugland, S. Oldknow, J. A. Cooper, M. J. Burke, A. Scott, W. Grantham, J. Vallejo, E. K. Brechin, P. J. Lusby and S. L. Cockroft, *Chem*, 2019, **5**, 1275–1292.
25 Y. You, K. Zhou, B. Guo, Q. Liu, Z. Cao, L. Liu and H.-C. Wu, *ACS Sens.*, 2019, **4**, 774–779.
26 H.-J. Schneider and A. K. Yatsimirsky, *Principles and methods in supramolecular chemistry*, Wiley, Chichester, 2000.
27 P. Thordarson, *Chem. Soc. Rev.*, 2011, **40**, 1305–1323.
28 L. You, D. Zha and E. V. Anslyn, *Chem. Rev.*, 2015, **115**, 7840–7892.
29 S. Sinn and F. Biedermann, *Isr. J. Chem.*, 2018, **58**, 357–412.
30 S. Sinn, J. Kramer and F. Biedermann, *Chem. Commun.*, 2020, **56**, 6620–6623.
31 J. Kim, I. S. Jung, S. Y. Kim, E. Lee, J. K. Kang, S. Sakamoto, K. Yamaguchi and K. Kim, *J. Am. Chem. Soc.*, 2000, **122**, 540–541.
32 S. J. Barrow, S. Kasera, M. J. Rowland, J. del Barrio and O. A. Scherman, *Chem. Rev.*, 2015, **115**, 12320–12406.
33 S. Sinn, E. Spuling, S. Bräse and F. Biedermann, *Chem. Sci.*, 2019, **10**, 6584–6593.
34 V. Maes, Y. Engelborghs, J. Hoebeke, Y. Maras and A. Vercruysse, *Mol. Pharmacol.*, 1982, **21**, 100–107.
35 Å. Frostell-Karlsson, A. Remaeus, H. Roos, K. Andersson, P. Borg, M. Hämäläinen and R. Karlsson, *J. Med. Chem.*, 2000, **43**, 1986–1992.
36 Y.-C. Liu, W. M. Nau and A. Hennig, *Chem. Commun.*, 2019, **55**, 14123–14126.
37 M. V. Rekharsky, Y. H. Ko, N. Selvapalam, K. Kim and Y. Inoue, *Supramol. Chem.*, 2007, **19**, 39–46.
38 A. L. Koner, C. Márquez, M. H. Dickman and W. M. Nau, *Angew. Chem. Int. Ed.*, 2011, **50**, 545–548.
39 Z. Miskolczy, M. Megyesi, L. Biczok, A. Prabodh and F. Biedermann, *Chemistry*, 2020, **26**, 7433–7441.
40 A. I. Lazar, F. Biedermann, K. R. Mustafina, K. I. Assaf, A. Hennig and W. M. Nau, *J. Am. Chem. Soc.*, 2016, **138**, 13022–13029.
41 S. Zhang, L. Grimm, Z. Miskolczy, L. Biczok, F. Biedermann and W. M. Nau, *Chem. Commun.*, 2019, **55**, 14131–14134.